

# Mechanical Performance of Laminated Veneer Lumber and Glulam Beams after Short-Term Incident Heat Exposure

Manuscript as Accepted in Construction and Building Materials

DOI: 10.1016/j.conbuildmat.2020.120129

(Manuscript Author order: Chorlton, Gales)



John Gales PhD (Principal Investigator, York University)  
Bronwyn Chorlton (Graduate Student, York University)

## Abstract

Timber use is becoming more appealing in the recent years especially ‘exposed timber’; however, the information available on the performance of engineered timber after fire is limited. This paper explores the performance of timber elements exposed to well defined thermal boundary conditions and examines the extent of adhesive degradation after heating. Two different types of timber beams are explored; ‘glued laminated timber’ (Glulam) and ‘laminated veneer lumber’ (LVL). A subset of beams was exposed to radiant heat as per a modified ASTM E1321 heating procedure. An additional subset of beams also had an area of their cross-section carved away, equivalent to the char depth of the heated beams. The carved beams allow for the identification of degradation beyond the char layer, as theoretically both the carved and charred beams would have the same effective cross-sectional area. All beams were mechanically loaded to failure using a four-point loading setup. While the current allowance for degradation beyond the char layer is considered to be 7 mm for exposure times of 20 minutes and greater [1], the results herein indicate that for bending members this layer extends to at least a minimum of 11.7 mm for LVL and 12.3 mm for Glulam. The aim of this paper is to assess the post-fire performance of Glulam and LVL through looking at strength loss due to adhesive degradation, which may contribute towards enabling tall and unencapsulated engineered timber buildings.

**Keywords:** Radiant heat, adhesive strength loss, fire design, timber, Glulam, Laminated Veneer Lumber.

## Table of Contents

Abstract.....	ii
1. Introduction and Motivation .....	1
2. Background .....	1
2.1 Current State of Practice .....	1
2.2 Previous Studies and Research Needs.....	2
3. Methodology .....	3
3.1 Specimens .....	3
3.2 Heating and Carving.....	5
3.3 Mechanical Loading .....	8
3.4 Deformation Measurement.....	9
4. Results and Discussion .....	9
4.1 Evaluation and Determination of the Zero-Strength Layer .....	14
4.2 Limitations and Future Research .....	15
5. Conclusion.....	17
Acknowledgements .....	17
References .....	17

## 1. Introduction and Motivation

The use of engineered timber, such as Glued Laminated timber (Glulam) and Laminated veneer lumber (LVL), is recently increasing especially in the construction of tall timber buildings, which is raising an urgent need to explore the fire resistance of such materials [2]. The thermo-mechanical performance of these materials under both standard and non-standard fire exposures should be explored to provide a better understanding of the material's potential for repair after a fire [3]. In terms of the quantity of resources required to return to an operable state, this research can help to demonstrate a timber building's ability to enable operational resilience to approval and insurance agencies [4,5]. Since the post-fire strength of the engineered timber has a significant impact on buildings, the strength-loss due to heat exposure of glued laminated timber (Glulam) and laminated veneer lumber (LVL) are explored in this paper using a very controlled heating setup which leads to a controlled damage state.

## 2. Background

### 2.1 Current State of Practice

The use of timber in tall buildings is challenging since timber is a combustible material [6–8]. Residual strength of the structural timber members after fire need to be understood to provide in depth guidelines for the designers. Current code allowances enable the calculation of the strength of an engineered timber member after fire [1]. The strength losses can be determined by calculating the char depth and adding an allowance for degradation effects known as the zero-strength layer. The remaining cross-section is considered to be undamaged. Char depth is typically calculated as a function of the time exposed to fire, and the type of timber in consideration. For Glulam and LVL, the charring rate is taken as 0.70 mm/min for notional charring, which accounts for effects such as corner rounding [1,9]. A visualization of the thermal degradation of wood can be seen in Fig. 1.

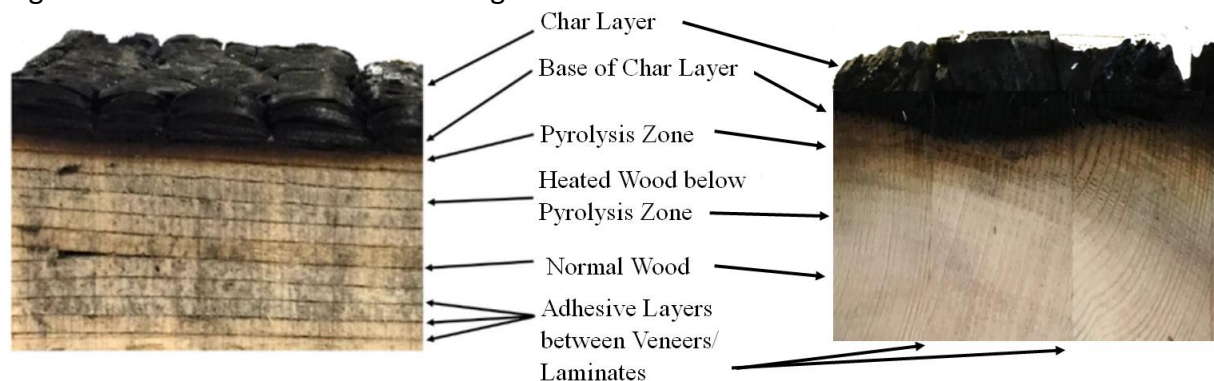


**Fig. 1** The charring and pyrolysis forming on fire-exposed timber (LVL is pictured left, Glulam pictured right. Timber depicted is different from timber tested and is only meant to illustrate charring and pyrolysis zones)

Current practices take the zero-strength layer as 7 mm for standard fires over 20 minutes and a proportionally smaller value for shorter exposure times [1,10,11]. The lack of confidence in these values adds to the uncertainty of the expected strength after a fire, and therefore how to

fully rationalize leaving engineered timber exposed [7,12,13]. It should be noted that while the research herein examines the post-fire performance of timber, the material properties (including at the pyrolysis layer) of timber may vary during high temperature exposure and following high temperature exposure. Previous studies have been performed to evaluate the adequacy of the zero-strength layer. Quiquero et al. [13,14] have examined the adhesive performance of 4.2 m long Glulam beams after fire under four-point bending. While the tests suggested that the zero-strength layer was inadequate, an additional finding was that significant material defects introduced variability into the results necessitating that future test programs expand the number of specimens being tested to account for variabilities in the wood itself.

## 2.2 Previous Studies and Research Needs

Currently, there is a need to study the effects of adhesive degradation in all types of engineered timber. To date existing research has focused on investigating the properties of 'cross laminated timber' (CLT) [3,6,8,15–18] with very limited studies on the effect of fire on other types of engineered timber such as LVL and Glulam [3,19,20]. The main outcome from investigating the effect of fire on CLT was that the fall-off of layers in fire may be a consequence of adhesive degradation [3,6,17]. Currently research is underway to improve engineered timbers performance in fire with the introduction of melamine based fire resistant adhesives (that are meant to not delaminate during standard fire tests).

Recent studies have shown that fire performance, and particularly charring of timber, is dependent on its physical properties more than the kinetics and chemical composition of different wood [21–23]. However, the fire performance can also partially be affected by the grain orientation, species, moisture content, and natural defects of the timber [22,24]. The structural fire performance of timber structures can be mainly dominated by its strength [25] and the adhesive between the timber layers therefore it is advised to avoid heating the adhesives [26]. However to date, there is not enough research to suggest a temperature limit, or an appropriate depth considered to be compromised [26].

To the author's knowledge, the study herein is one of the first of its kind to consider the adhesive degradation of LVL. The limited studies available regarding adhesive degradation (and the reduced cross section method) in Glulam include studies by Lange et al (2015) [12] and Schmid et al (2015) [27] (both out of the SP Technical Research Institute of Sweden). The study by Lange et al. (2015) considered two standard fire tests as well as two parametric fires, applied to 32 Glulam beams in total which were loaded to failure. Lange et al. (2015) found the zero-strength allowances to be unconservative, with their results showing a zero-strength layer of 8-16 mm is needed depending on the fire exposure [12]. The study by Schmid et al. (2015) considered five 140 x 269 mm Glulam beams subject to standard fire exposure and loaded in bending with a load that was maintained until failure. Schmid et al. (2015) suggested zero-strength layers of 9.5 mm to 20.1 mm in their study [27]. The findings of the studies by Schmid et al. (2015) and Lange et al. (2015) reinforce the need to study adhesive degradation, as clearly their results showed that the current zero-strength layer may not be conservative.

Quiquero et al. (2018) also looked at adhesive degradation in Glulam [13]. The study by Quiquero et al. (2018) consisted of small-scale Glulam samples heated in a Cone Calorimeter at varying heat exposures, and then mechanically loaded along the adhesive line to look at shear

strength. Quiquero et al. (2018) also looked at thin but long (4.2 m) Glulam beams in bending. Those beams were exposed to a pool fire on both sides, and then loaded in four point bending. The findings of Quiquero et al. (2018) concur with the above studies in that adhesive degradation may not be adequately accounted for in code procedures [13]. They also noted the need to study a high number of samples in attempt to reduce variability.

This study focuses only on the post-fire performance of under-studied Glulam and LVL samples. While in-fire performance is another aspect that could be considered, it is outside the scope of this study, as the goal is to improve the current understanding of engineered timbers resilience towards fire. A better understanding of the post-fire performance will be beneficial towards evaluating an engineered timbers potential for post-fire repair; and may help to enable the defensible implementation of exposed engineered timber in a structure.

### 3. Methodology

#### 3.1 Specimens

This study involved 18 LVL and 10 Glulam samples. A greater focus on LVL was considered as this material has been understudied as compared to other engineered wood products. Properties of the timber are seen in Table 1. The thickness of each laminate of the LVL was 3 mm, and the thickness of each Glulam laminate was 38 mm. Both specimens fall under the S-P-F (Spruce Pine Fir) species category. The Glulam beams were of Spruce species, while the LVL beams were of Pine species. All of the beams were damaged to the severity and in the locations described in Table 2 (where damage was incurred on both sides of the beams, while the tops and bottoms were left undamaged). It is seen from this table that two samples were observed for each damage state (ensuring repeatability).

**Table 1.** Timber material properties (from manufacturer's documentation)

Type	Bending Strength (MPa)	Shear Strength (MPa)	Modulus of Elasticity (MPa)	Density (kg/m <sup>3</sup> )	Moisture Content <sup>1</sup> (%)
LVL	39.5	3.8	13 790	569	10
Glulam	30.7	2.5	13 100	560	10

<sup>1</sup> Moisture content from author's measurement

The Glulam samples were cut from beams of original dimensions 45 (width) x 195 (height) x 4200 (length) mm. All Glulam beams were from the same production batch. The LVL samples were cut from beams of original dimensions 45 (width) x 241 (height) x 1829 (length) mm. All LVL beams were from the same production batch. Both the Glulam and LVL samples were cut to be 35 (width) x 155 (height) x 800 (length) mm for the heat exposure. These dimensions were selected to accommodate the Lateral Ignition and Flame Spread Test (LIFT) apparatus used for controlled heating. After heating, the height was cut to 75 mm (where no charring had occurred along the top or bottom of the member) prior to mechanical loading. This height which was chosen in order raise the span : depth ratio to be more representative of what has been observed in construction (for example the Mjøstårnet building in Norway [28]), while still preserving two

**Table 2.** Damage states and failure loads of all beams tested

Sample Number	Type	Damage State	Damage Region	Average Failure Load (kN)	Individual Failure Load (kN)	Standard Deviation (kN)
1	LVL	None (Control)	--	19.7	19.21	0.5
2					20.27	
3	LVL	Charred (5 mm)	Center	11.8	14.20	2.4
4					9.33	
5	LVL	Reduced Cross Section (5 mm)	Center	17.6	17.39	0.2
6					17.83	
7	LVL	Charred (5 mm)	Side	15.3	14.76	0.5
8					15.81	
9	LVL	Reduced Cross Section (5 mm)	Side	18.3	17.69	0.6
10					18.97	
11	LVL	Charred (10 mm)	Center	9.4	7.58	1.8
12					11.20	
13	LVL	Reduced Cross Section (10 mm)	Center	12.7	14.10	1.4
14					11.28	
15	LVL	Charred (10 mm)	Side	13.9	13.55	0.3
16					14.20	
17	LVL	Reduced Cross Section (10 mm)	Side	11.4	11.13	0.2
18					11.58	
19	Glulam	None (Control)	--	18.1	18.45	0.4
20					17.74	
21	Glulam	Charred (10 mm)	Center	14.8	15.97	1.1
22					13.64	
23	Glulam	Reduced Cross Section (10 mm)	Center	15.5	16.06	0.5
24					14.97	
25	Glulam	Charred (10 mm)	Side	13.1	16.41	3.3
26					9.87	
27	Glulam	Reduced Cross Section (10 mm)	Side	18.2	16.43	1.8
28					20.03	

adhesive layers in the Glulam (note that as the damage was only inflicted along the two sides of the beams, there was no significant damage along the top or bottom of the beam prior to reducing the height). The beams were all selected to be relatively free of defects, apart from small knots (which did not appear to alter the char depth or failure modes of the specimens). The Glulam laminates were joined together by finger joints (which again did not seem to impact charring or failure modes of any of the beams).

Two char depths were selected, 5 mm of char per side and 10 mm of char per side. The severe damage state of 10 mm was chosen so that it would theoretically have effectively no remaining cross-section after heating as per CSA O86. The original width of the samples was 35 mm, subtracting 10 mm of char depth and 7 mm of zero-strength layer per side, there would theoretically only be 1 mm of 'undamaged' cross-section remaining (approximately 0 mm, as each char depth was +/- 1 mm). 5 mm was chosen arbitrarily to be half of this char depth, as a point of comparison.

The 5 mm or 10 mm of controlled damage (produced by heat exposure or mechanical carving as described in the 'Heating and Carving' section below) was applied in two different locations along the beams. The first location is a 100 mm length in the center of the beam, with 350 mm of undamaged length on either side. This was chosen as it is in the center of the region of maximum moment and zero shear, when tested in four-point bending. The second location began 83 mm away from one end of the beam, for a damaged length of 100 mm. This is the center of one of the side thirds of the beam. This location is the center of the region of maximum shear, with an average amount of moment, when tested in four-point bending. These locations allow for an evaluation of the performance of the members in bending, and in shear. The length of the damaged region of the beam was selected as 100 mm because this length is small enough to obtain uniform damage when exposed to the radiant heater, while large enough to create a significant damage state.

The LVL samples contained phenol formaldehyde adhesive, while the Glulam contained a polyurethane-based adhesive. These materials were procured from local manufactures in the Ottawa, Canadian region. They would be typical of recent Canadian construction in Ontario. The LVL was manufacturer specified of the grade 2.0e - 3100Fb (graded in accordance with ASTM D5456-19 [29]). The Glulam samples were of the grade 24f-ES (graded in accordance with CSA O122-16 [30]). The flexural strength of the control beams was calculated from the four-point bending test to be 70 MPa for the LVL and 64 MPa for the Glulam (unfactored and determined from the maximum bending moment, and section dimensions). The modulus of elasticity calculated as 14 133 MPa for the LVL and 17 427 MPa for the Glulam (unfactored and determined from the beam deflection, and section dimension).

All samples were allowed to acclimatize to the laboratory conditions at 50% relative humidity and approximately 20°C for several months.

### 3.2 Heating and Carving

The damage was created using two procedures. The first procedure was charring using a LIFT apparatus as per a modified ASTM E1321 [31], and the second was by mechanically carving away a portion of the cross-section. The purpose of using the LIFT radiant heater apparatus for



the charring procedure was to obtain a well-controlled and repeatable damage state between tests. It should be noted that the pilot burner was not used. This was because the purpose was not to measure or propagate flame spread across the beam, only to use radiant heat to achieve a specific char depth. Additionally, the holder of the beams within the LIFT apparatus was modified so as to only expose specific regions (in the center or the side) of the beam to heat. Multiple ceramic boards designed to prevent heat penetration were placed in front of the engineered timber samples in locations where char depth was not desired. This is seen in Fig. 2. This configuration ensured that only the exposed portion of the beam would be damaged. The adhesive lines in the Glulam were parallel to the heat flux while the adhesive lines in the LVL were perpendicular to the heat flux (orientation of the specimens was retained from the original beam orientation). The Glulam was only one laminate thick, therefore the Glulam beams did not have any adhesive lines perpendicular to the heat flux. The angle of the radiant heater was left unchanged from ASTM E1321 specifications, where it is placed closest to the member near the side and angled 15 degrees away towards the middle.

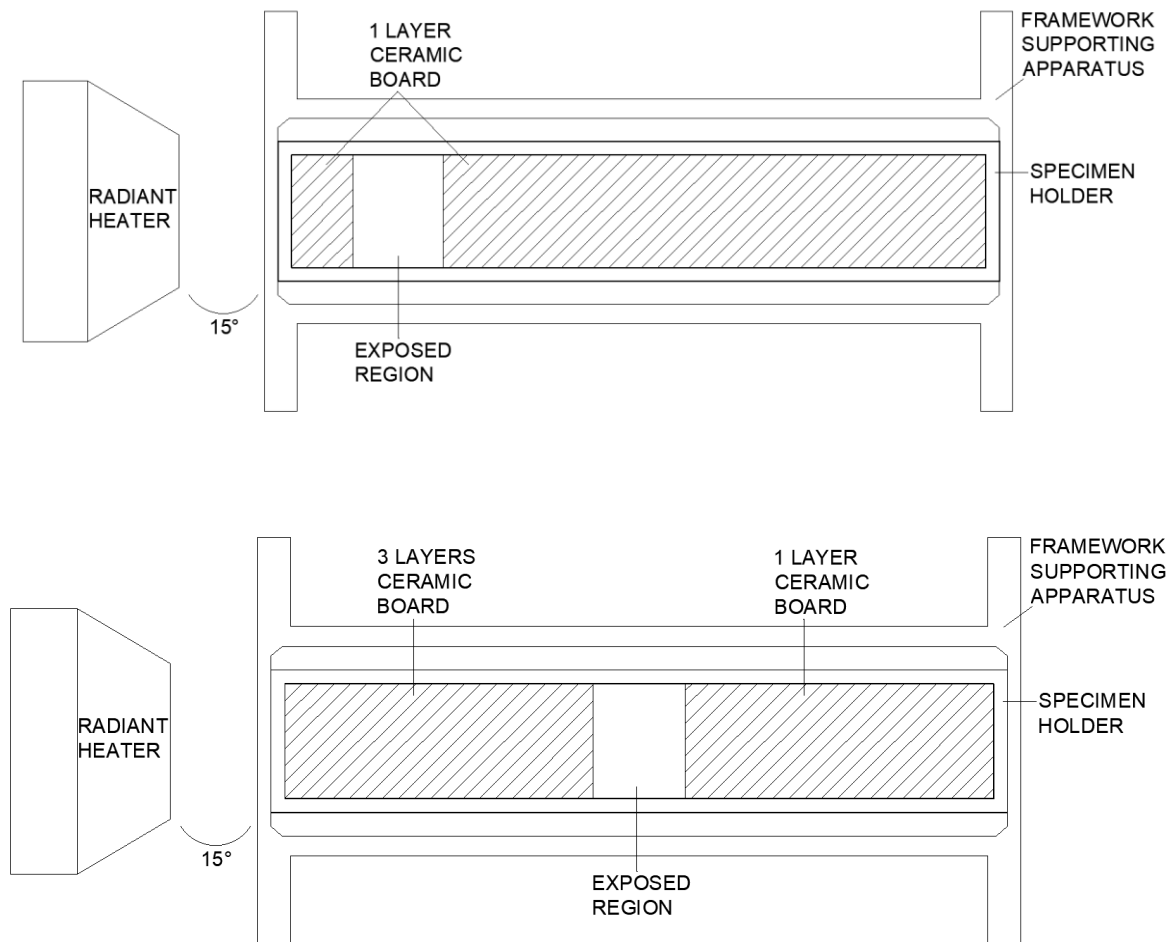


**Fig. 2** The heating test setup for the beams damaged in the shear region (top) and the moment region (bottom)

Due to the extended exposure duration of the beams exposed in the center, three layers of ceramic board were used for the moment damaged beams instead of the one layer that was otherwise needed, to ensure no damage was created where it was not desired. The extra boards were fastened externally to the holder (using Nickel-Chromium wire).

One consequence of placing ceramic boards in front of the engineered timber samples is that the samples were approximately 12 mm (the width of the ceramic board) further away from the radiant heater than typical. This caused the heat flux to vary slightly from its usual capacity. A calibration was performed to determine the heat flux that would result from an offset of 12 mm. The results can be seen in Fig. 3. This figure also displays the prescribed error of the LIFT apparatus heat flux gauge, which is taken as 10% of the incident heat flux.

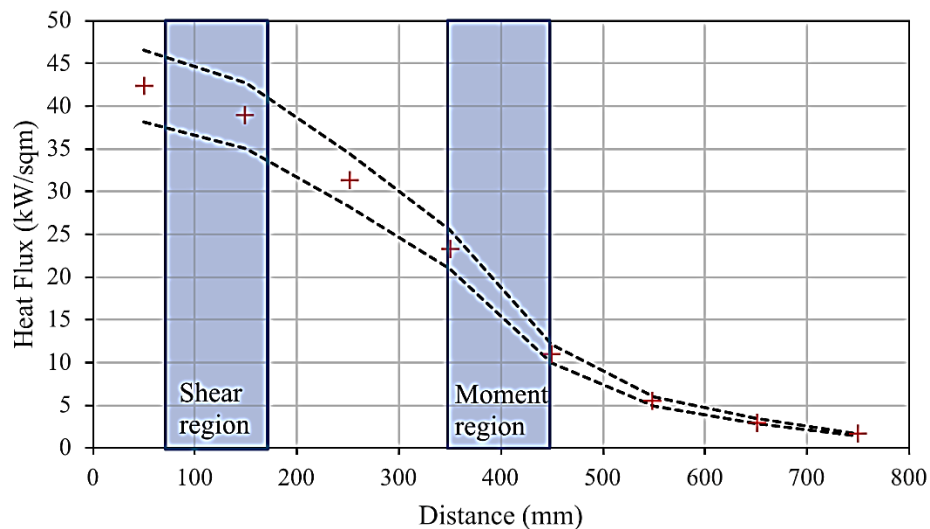


**Fig. 3** Heat flux measured by LIFT apparatus after an offset of 12 mm was applied, with the error of the apparatus displayed as contour lines

A consistent char depth was achieved in varying locations along the lengths of the beams by exposing them to the radiant heater for varying amounts of time. This method was selected over an alternative procedure of altering the distance of the radiant heater so that it would be parallel with the test specimen. The reason this method was avoided was that it significantly alters the standardized test conditions of the LIFT and impacts the studies reproducibility. Future research could explore more customized uses of radiant heaters as has been done by others [32]. One implication of this test setup is that the members damaged in the shear and moment regions were exposed to heat for varying lengths of time, since the radiant panel is initially closer to the end of the member and angled away from the member in the middle. While the differences in fire duration and distance from the member to the radiant panel may create some variation in the overall heat exposure, this test setup achieves a consistent and repeatable char depth. Using varying heat severities and exposure durations may create differences in the degradation of the timber (even if the same char depth is obtained), however at this time these mechanisms are not well understood and are in need of future research.

The exposure durations were determined by using trial samples of LVL and Glulam in the LIFT apparatus for varying amounts of time. These trial beams were cut in the regions of interest and the char depth was measured, to ensure a consistent char depth across the length of the

exposed region. While the beams were exposed to a slightly different heat flux along their exposed length, the char depth observed is relatively uniform ( $\pm 1$  mm across the area of interest).

In this test setup, the damage severity may be somewhat dependent on the ventilation conditions [33]. While the exact ventilation conditions may be difficult to replicate, the purpose of the test setup is to achieve a set amount of damage, and future researchers could alter the heat flux and exposure as needed to achieve the required damage state (measured in this paper by char depth). Though it is possible that otherwise identical damage states may have microstructural differences dependent on their heat flux and duration, as per the current state of knowledge, this has not been confirmed and there is little information available on these aspects.

The heat flux of the radiant panels reaches a maximum of 50 kW/m<sup>2</sup> (the heat flux along the entire length of the beam is seen in Fig. 3). While a real fire will be more severe than 50 kW/m<sup>2</sup>, these small-scale tests will still give an indication of the adequacy of the values used for the zero-strength layer. Moreover, this test series primarily examines the strength remaining given a particular damage state (char depth) and attempts to assess whether current code procedures are conservative given the damage, not the severity of the heat exposure.

The result of this heating procedure was that a consistent char depth was produced across all samples. This was achieved by carefully controlling several aspects within the procedure; such as the use of a radiant panel (as opposed to a pool fire or other type of heat exposure) that generated a consistent heat flux during each exposure. All other aspects of the testing environment remained constant between tests (such as ventilation conditions). The smaller beams that were tested, were cut from fewer larger beams, ensuring relatively consistent density, and were inspected to be relatively free of defects. For each of the damage states, trial specimens were used to determine the exact duration of heating needed to create the desired damage state. The result was a very consistent heat exposure induced on very similar beams across the intended heated region, which generated a reasonably controlled char depth. The authors observed each specimen to ensure the char depth was either 5 mm or 10 mm as desired ( $\pm 1$  mm due to author's interpretation of the initiation of the pyrolysis zone).

### 3.3 Mechanical Loading

At this stage, the char depths of the charred beams were measured and confirmed. Mechanical loading occurred at a rate of 2.5 mm/min, in line with the loading rate used for ASTM D143 for four-point bending tests [34]. A load actuator applied two-point loads onto the simply supported beams. The total span of the beam was 800 mm. The ends of the beams were aligned with the centre of the supporting rollers, with a small plate that could rotate freely in between the roller and the beam. This setup negated the need for the beam to overhang past the support (such that the beam length and span are both 800 mm). The setup of the mechanical loading procedure can be seen in Fig. 4. All beams were loaded to failure. The damaged areas of the beams were oriented to be on the two sides of the beam, and not on the top and bottom.

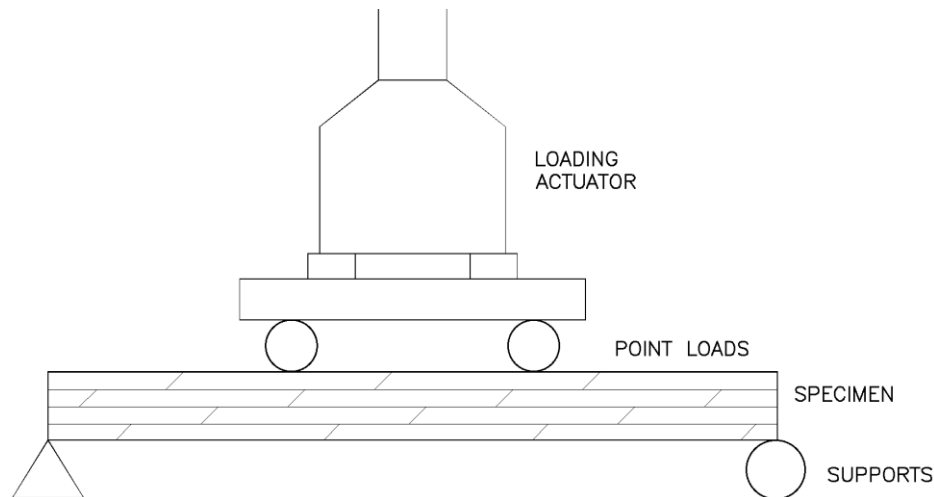


**Fig. 4** The four-point bending test setup (where Glulam is depicted, and damaged regions would be on the front side and back side of the beams, with the top and bottom being undamaged)

### 3.4 Deformation Measurement

The deformation of the beams was measured using Digital Image Correlation (DIC), and specifically GeoPIV RG software [35]. This method was selected over using traditional strain gauges. This software has been proven to be accurate in the measurement of strain and displacement of wood with an error of 0.15 pixels [14,36].

GeoPIV RG software is able to observe specific patterns located on the beam and measure their displacement. These unique patterns are created by painting a speckled pattern on the beams. For these tests, black paint was used on the uncharred timber and white paint was used on the charred portion, to create a high contrast pattern for the software to track. High-resolution photographs were taken at five-second intervals using a Canon EOS-5Ds camera. For this test series, DIC was primarily used to measure deformation at the center of the beam.

## 4. Results and Discussion

All of the beams failed while they were tested in four-point bending. The average failure loads for each type of damage is seen in Table 2. The LVL has been divided into its two damage states (5 mm and 10 mm) for this analysis. The failure loads of both sets of LVL beams and the Glulam can be seen in Fig. 5. The vast majority of the beams experienced a tension failure within the moment region. The carving process did not reach a very substantial depth, and therefore no significant local stresses were created.

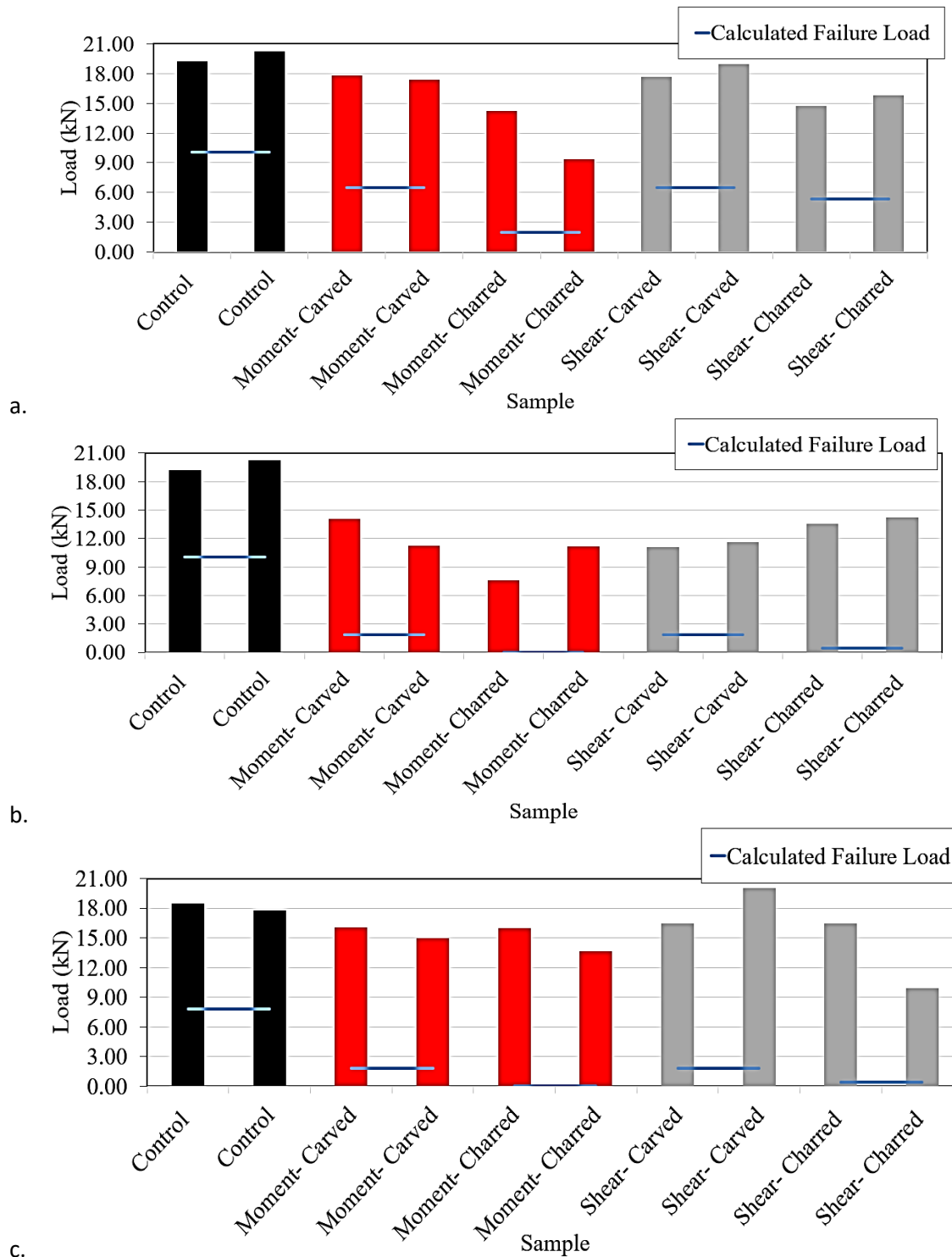


**Fig. 5.** Failure loads for all beams, a. LVL at the 5 mm char depth, b. LVL at 10 mm char depth, and c. Glulam at 10 mm char depth

Displayed in Fig. 5 is the calculated failure load of each beam, as per CSA O86. The beams with 10 mm char have a predicted failure load of approximately 0 kN. This is due to a significant reduction in predicted strength due to lateral stability as the effective width is very small. As the

purpose of this test program is not to evaluate the accuracy of the current procedures for calculating char depth, the measured char depth has been used (either 5 mm or 10 mm) in the prediction of the charred beams' failure load. A calculated zero-strength layer has been added to the actual char depth, and the predicted capacity has been calculated based on the remaining cross-section. The zero-strength layer is taken as 7 mm for exposures of 20 minutes or greater in duration, and proportionally less for exposure times of less than 20 minutes [1]. The predicted strength of both the carved beams and the charred beams takes into account the reduction in cross-section, however only the predicted strength of the charred beams considers the effect of the zero-strength layer. In all cases, the beams performed significantly better than predicted. Properties used in the strength calculations are seen in Table 1.

For the most part, the LVL 5 mm damage state beams performed as expected. For both the beams damaged in the moment and shear regions, the carved beams carried more load than the charred damaged beams. When compared to the control beams, the charred moment beams had their capacity reduced an average of 40%, while the charred shear beams had their capacity reduced an average of 22%. This indicates that, for LVL, the moment capacity may be more sensitive to thermal degradation of the adhesives than the shear capacity. As the structure of LVL is composed of layers of thin vertical laminates (where the adhesive layers are oriented vertically, parallel to the application of the load), that individually have little moment capacity, it may be more important that the adhesives hold the laminates together to create a single composite unit, which has significant moment capacity. This may be less important for shear.

The LVL beams carved in the shear region displayed differing results between the 5 mm and 10 mm damage states. For the 5 mm damage in the shear region, the carved beams failed at a higher load than the charred beams. The opposite is true for the 10 mm damage state. The reason the carved beams failed at a lower failure load than anticipated may be that the carving of the beams causes the full width of a number of the laminates to become exposed. As a result, the failure mode that is observed is that the laminates that have become detached fail earlier than the rest of the cross-section. This failure mode can be seen in Fig. 6. This is less of an issue for the less severely damaged beams, as fewer of the layers of laminates have become exposed during the carving process.



**Fig. 6** Failure of an LVL beam, carved to the 10 mm damage state (carved area seen on the left-hand side of beam, bound by the split in the wood, and the support)

Similar to the LVL, the observed failure loads of Glulam were significantly higher than the calculated failure loads. The failure loads of the Glulam beams show that the charred moment beams did not have their capacity significantly reduced compared to the carved beam; on

average, the failure load was only lowered by 0.71 kN (4.6%). The beams charred in the shear region were more impacted by the heating. The beams charred in the shear region experienced an average failure load of 5.09 kN lower than the carved beams (27.9%). The finding that the beams damaged in the shear region had their capacity reduced significantly more than the beams damaged in the moment region is consistent with previous studies [13]. Contrary to the LVL, the laminates within the Glulam are adhered together in horizontal layers (such that adhesive layers are perpendicular to the load). In a larger Glulam section, more laminates would be joined with vertical adhesive lines to increase the thickness, however in these sections the thickness consisted of only one laminate and therefore no vertical adhesive lines are present. This orientation is in line with the orientation of the original beam sections from which the samples were extracted and may explain some differences between the performance of the LVL and the Glulam.

DIC was used to plot the load versus displacement curves for all the beams. These graphs may be seen in Fig. 7. One of the LVL shear beams charred to 5 mm in the shear region had its capacity drop suddenly a number of times (denoted by Sample #8 – Charred). This beam failed by gradually deflecting, and ultimately cracking in its damaged region. This was also the failure mode for the other charred beam, though they did not exhibit such a sudden failure. This discrepancy may be explained a possible material defect within the LVL, causing it to fail at a lower load than expected.

The slope of the load-displacement curves of the LVL beams carved to 10 mm in the shear region (Fig. 7b) begin similarly to the charred and controlled beams, but they eventually begin to plateau. This represents the point at which the outer laminates fail (the failure mode seen in Fig.6), though the remainder of the beam is still able to carry some load. Also notable is that the load versus displacement curves for the Glulam (Fig. 7c) show that one of the beams charred in the shear region (Sample #26 – Charred) experienced a number of drops in its carried load. The initial drop occurs upon initiation of a crack within the shear region. The following drops represent the growth of this crack, which ultimately led to its failure.

These results show differences between the performance of the Glulam and LVL beams. The Glulam was more impacted by the heating in the shear region, while the LVL was more impacted in the moment region. This may due to the inherent properties of the timber and how it is fabricated. The moment capacity of Glulam may be less reliant on the adhesive strength and rather reliant on the strength of the wood itself, whereas the finger joints of the Glulam may be more vulnerable to shear. As mentioned earlier regarding the LVL, it may be more important for each layer of laminate to act together as a single unit to withstand moment, as individually each laminate has little moment resistance but together, they have significant resistance. For this reason, the performance of the adhesives may be more significant in the moment region than the shear region.

Other differences in the performance of the LVL and Glulam beams may also be attributed to their material differences, as the Glulam and LVL beams were made of differing timber species and have different material properties [37]. The adhesives used in each timber type were also different, with Glulam using a polyurethane based adhesive and LVL using a phenol formaldehyde based adhesive. The two adhesives will perform differently when heated, which may further contribute to any variation between the results of the Glulam and LVL.



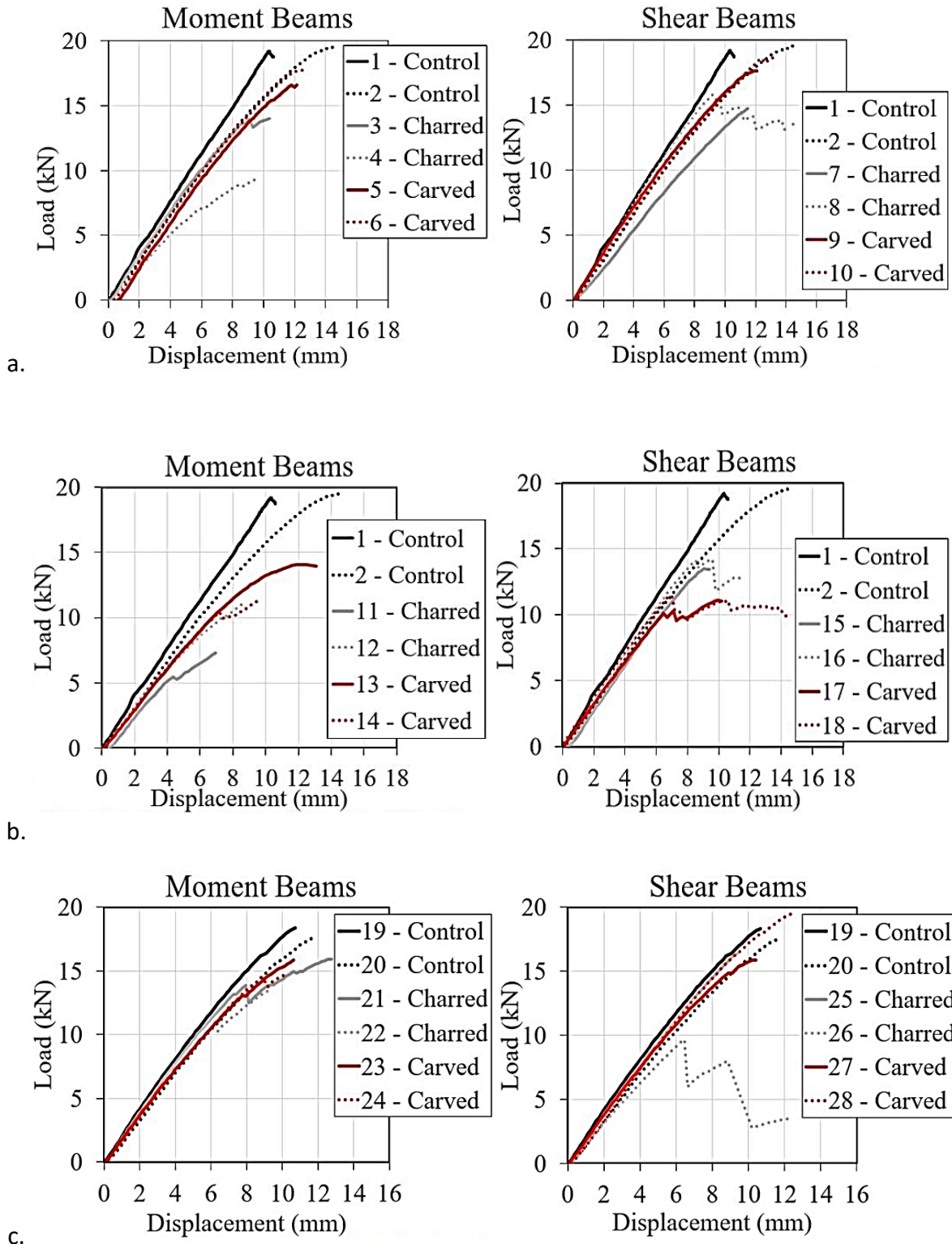


**Fig. 7** Load versus displacement curves a. LVL at the 5 mm char depth, b. LVL at 10 mm char depth, and c. Glulam at 10 mm char depth



#### 4.1 Evaluation and Determination of the Zero-Strength Layer

The differences between the carved and charred beams, as observed and as predicted, may be seen in Table 3. In a number of cases, the observed difference in strength is larger than the calculated difference in strength. This is indicative that the allowance for the zero-strength layer may not be conservative in accounting for strength loss for all cases.

**Table 3.** The difference between the failure loads of the carved and charred beams, as observed and as calculated by CSA O86-14

Type	Damage Severity (mm)	Location	Observed Difference (kN)	Observed charred beam capacity/carved beam capacity (%)	Calculated Difference (kN)	Calculated charred beam capacity/carved beam capacity (%)
LVL	5	Moment Region	5.84	66.8	4.49	30.6
LVL	10	Moment Region	3.30	74.0	1.90	0.0
LVL	5	Shear Region	3.05	83.4	1.11	82.8
LVL	10	Shear Region	-2.52	122.2	1.90	24.7
Glulam	10	Moment Region	0.71	95.4	1.80	0.0
Glulam	10	Shear Region	5.09	72.1	1.36	24.4

The revised zero-strength layers were determined by calculating the beam width that would correspond to the observed difference in failure load between carved and charred beams, for each case in Table 3 where the observed difference exceeds the calculated difference. While standards such as CSA O86 and Eurocode 5 [1,10] linearly reduce their suggested zero-strength layers for exposure times less than 20 minutes, this has not been done due to the short exposure times, and therefore the zero-strength layers discussed herein should be considered an absolute minimum value. The results suggest that a minimum zero-strength layer of 11.7 mm would be needed for the LVL, and 12.3 mm would be needed for the Glulam.

In comparison to studies done by other researchers, the results for the Glulam beams are similar to the results observed by Quiquero et al. [13] (Quiquero et al. did not study LVL so no comparison can be made to that study). Similar trends were observed in that the capacity of the beams damaged in the moment region were not as severely impacted by fire exposure as the beams damaged in the shear region. The findings of Quiquero et al. [13] also showed that the calculated residual strength was lower than the actual strength in all cases, however, the difference in observed capacity between the carved and charred beams was not adequately accounted for by allowances for the zero-strength layer.

Quiquero et al. (2018) have suggested the use of a zero-strength layer of 23 mm, compared to 12.3 mm found for Glulam in this study. Factors that may account for this discrepancy are that the first phase of the tests performed by Quiquero et al. (2018) utilized 100

x 100 mm samples, tested using an apparatus meant to shear the specimen along the adhesive line. This mode of loading intentionally created failure at the adhesive line, presumed to be the weakest part of the specimen. This loading setup was significantly different from the four-point bending test setup used in this test series where combined forces will act on adhesive lines. The second phase of tests performed by Quiquero et al. (2018) occurred on 4200 x 195 x 45 mm beams. These beams were significantly larger than the beams tested within this test program and were therefore more likely to contain a defect that is not visible. These defects could significantly reduce the strength of these beams, therefore implying a larger zero-strength layer. Moreover, these larger beams failed frequently along the finger joints, and the larger beams had a higher quantity of these joints than their smaller counterparts. Finally, the larger beams were loaded using an apparatus that restrained the beams laterally at the supports, but only restrained the beams laterally at quarter span until halfway down the depth of the beam. This may have allowed for some degree of lateral-torsional buckling to occur that was not present with the smaller sample size as seen within this test program, causing an earlier failure.

Additional tests by other researchers which offer a revised value for the zero-strength layer include the study by Schmid et al. (2015), which considered Glulam members in tension, compression, and bending [27]. In terms of the members in bending, Schmid et al. (2015) found the zero-strength layer to range from 9.5 mm to 20.1 mm. Lange et al. (2015) found the zero-strength layer to range from 8 mm to 16 mm dependent on the type of heat exposure [12]. The zero-strength layer proposed by the authors of this paper for Glulam of 12.3 mm has relatively good agreement with the range of values proposed by both Schmid et al. (2015) and Lange et al. (2015).

CLT is a comparable timber product for which researchers have also proposed revised zero-strength layers. Wiesner et al. found the zero-strength layer of CLT walls to be between 15.2 mm and 21.8 mm [38]. This is slightly higher than the zero-strength layers previously found in this paper, however this could be due to the type of timber product considered. This may be the case due to differences in additives that may be unique to each product, or that the configuration of timber laminates and adhesives may also play a role. The large size of the CLT walls tested by Wiesner et al. (2017) will, as previously mentioned, also introduce increased potential for material defects or more complex failure mechanisms than the small beams considered in this paper.

The LVL examined in this test series is, to the authors' knowledge, the first study to investigate adhesive degradation in LVL through controlled tests, so there are presently no previous studies to compare suggested zero-strength layers. It is apparent, however, that adhesive degradation is present in LVL. Although the factors outlined in the above paragraph assist in understanding the variation in different author's proposed zero-strength layers, all the studies discussed concur that the 7 mm currently used as the thickness of the zero-strength layer does not adequately account for degradation effects in all cases.

#### 4.2 Limitations and Future Research

The tests described above provided significant insight as to the adhesive performance of Glulam and LVL beams post-fire. These tests have helped to identify a number of future research topics that would aid to further understand the extent of the adhesive degradation.

The small size of the beams and the relatively short exposure times considered within this test program is one constraint that could be addressed in future research. For beams exposed to fire than less than 20 minutes, standard procedures suggest reducing the zero-strength linearly according to time exposed [1,10], however this has not been done in the calculation of the zero-strength layer due to the short heating times, and therefore the zero-strength layers suggested by this paper are an absolute minimum value. It would therefore be beneficial to perform tests with longer heat exposures. Moreover, the small size of the beams resulted in predicted failure loads being largely reduced due to lateral stability concerns. Tests with larger cross-sections may be affected less by this consideration. It would be beneficial if the larger scale tests utilized members that were of a cross-sectional area representative of what would typically be used in construction (realistic scale), which would negate lateral-torsional buckling effects that may occur.

Moreover, the adhesives used for the LVL and Glulam samples featured in the test series were phenol formaldehyde and polyurethane-based, respectively. These adhesives vary between manufacturers and are constantly evolving in material design, so it would be beneficial to understand the post-fire performance of a wide number of specific adhesives. As new adhesives are developed, additional testing will be required to understand how these perform post-fire.

The upper end of the heat flux emitted by the radiant heater in these tests was around 50 kW/m<sup>2</sup>. Other fire exposures, including to standard time temperature curves such as CAN/ULC S101 [39] or ISO 834 [40], will expose the timber to different heat fluxes which may result in a different size of pyrolysis zone. The required zero-strength layer may therefore vary according to heat flux. The damage applied to the beams in this test series varied from what is likely to be observed in a real fire in that the bottom of the beams were not damaged. As the beam height is an important factor in determining residual strength, and if the bottom of the beam were exposed to fire the strength may have been more greatly reduced, this difference between these tests and a real fire must be considered.

It is important to note that the zero-strength layer will be dependent on the particular geometry of members, the specific material properties, and fire duration and severity (to name just a few factors which can affect overall fire performance). More research is needed in the development of a method in determining zero-strength layers in these different scenarios. The research study described in this paper reinforces the notion that a 7 mm zero-strength layer is not always conservative and highlights the need for future research. While this study has begun to address some of the research needs identified previously, future research described in the above paragraphs would further help to fulfil the objectives outlined by Yang et al. [25], such as gaining acceptance of design guides. It would also help to address knowledge gaps as identified by [26] such as defining a depth of material affected by the degradation of adhesives at elevated temperatures. Additional future research topics could address the degradation of adhesives at high temperatures from a material chemistry perspective. This would be beneficial in understanding the deterioration mechanisms of the adhesives, especially as new adhesives continue to be developed.

## 5. Conclusion

A comprehensive understanding of the Glulam and LVL's post-fire performance is critical to provide a safer approach in designing tall timber buildings. Understanding their post-fire performance will also be beneficial in enabling the ability to leave engineered timber exposed without encapsulation, fulfilling architectural desires. For these objectives to be implemented there is a need to evaluate the current procedures for determining the losses due to adhesive degradation.

The results demonstrated that loss in strength beyond the char layer occurs when the beams are exposed to fire, as observed by comparing the carved and charred beams. The LVL experienced a larger loss in strength for the beams damaged in the moment region, failing on average at 70% of the capacity the mechanically carved beams. The Glulam beams observed a different trend, with the beams damaged in the shear region experiencing a larger reduction in strength, failing on average at 72% of the capacity of the mechanically carved beams. This difference in the performance of the two timber types may be due to the inherent differences in their macro-structures (including differences in the configurations in which Glulam and LVL are assembled).

The existing zero-strength layer guidance of 7 mm for exposures of 20 minutes and greater was found to not conservatively account for losses due to adhesive degradation. For the LVL tested in this series, a minimum zero-strength layer of 11.7 mm may be required to be able to adequately account for losses due to adhesive degradation. For the Glulam beams tested in this series, a minimum zero-strength layer of 12.3 mm would be required to adequately account for losses due to adhesive degradation. These values for the zero-strength layer may not be conservative for larger-scale beams and in many other cases where the heat exposure, member geometry, material properties, etc. may vary. Further testing is required to determine a more appropriate value in these cases. Nevertheless, these results make it clear that for both LVL as well as Glulam, a 7 mm zero strength layer is not always conservative. These findings reinforce the need to better understand the severity of degradation beyond the char layer in a variety of commonly used engineered timber types through additional full-scale tests and further research into adhesive development, in order to enable the construction of tall and unencapsulated timber structures.

## Acknowledgements

The authors appreciate the funding provided through NSERC USRA, CGS, York University, and NSERC Discovery Grant RGPIN-2015-05081. Thank you to Rwayda Al Hamd and Chloe Jeanneret for their technical contributions.

## References

- [1] CSA Group, CSA O86-14: Engineering Design in Wood, 2014.
- [2] D. Barber, Determination of fire resistance ratings for glulam connectors within US high rise timber buildings, *Fire Saf. J.* 91 (2017) 579–585. doi:10.1016/j.firesaf.2017.04.028.

- [3] J. ichi Suzuki, T. Mizukami, T. Naruse, Y. Araki, Fire Resistance of Timber Panel Structures Under Standard Fire Exposure, *Fire Technol.* 52 (2016) 1015–1034. doi:10.1007/s10694-016-0578-2.
- [4] M. Smith, J. Gales, Enabling operational resilience through performance-based fire design, in: 6th Int. Struct. Spec. Conf. CSCE Annu. Conf., Vancouver, BC, 2017.
- [5] B. Chorlton, G. Harun, E. Weckman, M. Smith, J. Gales, An Investigation into the Resilience of Glulam Timber Beams after Fire Exposure, in: 7th Int. Struct. Spec. Conf. CSCE Annu. Conf., Fredericton, NB, 2018.
- [6] R. Crielaard, J.-W. van de Kuilen, K. Terwel, G. Ravenshorst, P. Steenbakkers, Self-extinguishment of cross-laminated timber, *Fire Saf. J.* 105 (2019) 244–260. doi:10.1016/j.firesaf.2019.01.008.
- [7] J. Schmid, J. König, A. Just, The Reduced Cross-Section Method for the Design of Timber Structures Exposed to Fire- Background, Limitations and New Developments, *Struct. Eng. Int.* 22 (2012) 512–522. doi:10.2749/101686612X13363929517578.
- [8] R. Emberly, A. Nicolaidis, F. Dillum, J. Torero, Changing Failure Modes of Cross-Laminated Timber, in: 9th Int. Conf. Struct. Fire, Princeton, NJ, 2016.
- [9] J. König, Notional versus one-dimensional charring rates of timber, in: 8th World Conf. Timber Eng., Lahti, Finland, 2004: pp. 483–486.
- [10] CEN EC5 1.2, European Committee for Standardization, Eurocode 5 – Design of timber structures Part 1-2: General – Structural fire design, Eurocode 5 – Des. Timber Struct. (2004).
- [11] E.L. Schaffer, C.M. Marx, D.A. Bender, F.E. Woeste, Research Paper 467: Strength Validation and Fire Endurance of Glued-Laminated Timber Beams, Madison, WI, 1986.
- [12] D. Lange, L. Bostrom, J. Schmid, J. Albrektsson, The Reduced Cross Section Method Applied to Glulam Timber Exposed to Non-standard Fire Curves, *Fire Technol.* 51 (2015) 1311–1340. doi:10.1007/s10694-015-0485-y.
- [13] H. Quiquero, B. Chorlton, J. Gales, Performance of Adhesives in Glulam after Short Term Fire Exposure, *Int. J. High-Rise Build.* 7 (2018) 299–311. doi:10.21022/IJHRB.2018.7.4.299.
- [14] H. Quiquero, J. Gales, Behaviour of Fire Damaged Engineered Timber Beams, in: 5th Int. Struct. Spec. Conf. Can. Soc. Civ. Eng., London, ON, 2016: pp. 993–1001.
- [15] J. Su, P. Lafrance, M. Hoehler, M. Bundy, Fire Safety Challenges of Tall Wood Buildings – Phase 2: Task 2 & 3 – Cross Laminated Timber Compartment Fire Tests, Quincy, MA, 2018. doi:https://doi.org/10.18434/T4/1422512.
- [16] D. Brandon, C. Dagenais, Fire Safety Challenges of Tall Wood Buildings – Phase 2: Task 5 – Experimental Study of Delamination of Cross Laminated Timber (CLT) in Fire, 2018.
- [17] S. Zelinka, S. Pei, N. Bechle, K. Sullivan, N. Ottum, D. Rammer, L. Hasburgh, Performance of Wood Adhesives for Cross-Laminated Timber Under Elevated Temperatures, in: World Conf. Timber Eng., Seoul, Republic of Korea, 2018.
- [18] H. Quiquero, J. Gales, R. Al Hamd, A. Abu, Finite Element Modelling of Post-tensioned Timber Beams at Ambient and Fire Conditions, (2019) 1–31. doi:10.1007/s10694-019-00901-0.
- [19] B. Subyakto, T. Hata, I. Ide, S. Kawai, Fire-resistant performance of a laminated veneer lumber joint with metal plate connectors protected with graphite phenolic sphere sheeting, *J. Wood Sci.* 47 (2001) 199–207.

- [20] M. Fragiaco, A. Menis, P.J. Moss, I. Clemente, A.H. Buchanan, Numerical and experimental thermal-structural behaviour of laminated veneer lumber (LVL) exposed to fire, 11th World Conf. Timber Eng. 2010, WCTE 2010. 4 (2010) 3047–3056.
- [21] W. Lane, A.H. Buchanan, P.J. Moss, Fire performance of laminated veneer lumber (LVL), World Conf. Timber Eng. (2004).
- [22] A.I. Bartlett, R.M. Hadden, L.A. Bisby, A Review of Factors Affecting the Burning Behaviour of Wood for Application to Tall Timber Construction, *Fire Technol.* 55 (2019) 1–49. doi:10.1007/s10694-018-0787-y.
- [23] F. Richter, A. Atreya, P. Kotsovinos, G. Rein, The effect of chemical composition on the charring of wood across scales, *Proc. Combust. Inst.* 37 (2019) 4053–4061. doi:10.1016/j.proci.2018.06.080.
- [24] M.J. Spearpoint, J.G.J. Quintiere, Predicting the burning of wood using an integral model, *Combust. Flame.* 123 (2000) 308–325.
- [25] J.C. Yang, M. Bundy, J. Gross, A. Hamins, F. Sadek, A. Raghunathan, NIST Special Publication 1188: International R&D Roadmap for Fire Resistance of Structures Summary of NIST/CIB Workshop, 2015. doi:10.6028/NIST.SP.1188.
- [26] Fire Protection Committee of the Structures Engineering Institute of the American Society of Civil Engineers, *Structural Fire Engineering*, Reston, Virginia, 2018. doi:https://doi.org/10.1061/9780784415047.
- [27] J. Schmid, A. Just, M. Klippel, M. Fragiaco, The Reduced Cross-Section Method for Evaluation of the Fire Resistance of Timber Members: Discussion and Determination of the Zero-Strength Layer, *Fire Technol.* 51 (2015) 1285–1309. doi:10.1007/s10694-014-0421-6.
- [28] R. Abrahamsen, Mjøstårnet-Construction of an 81 m tall timber building, *Int. Holzbau-Forum IHF.* (2017) 12.
- [29] ASTM International, ASTM D5456-19 Standard Specification for Evaluation of Structural Composite Lumber Products, West Conshohocken, PA, 2019.
- [30] CSA Group, O122-16: Structural glued-laminated timber, Toronto, Ontario, 2016.
- [31] ASTM International, ASTM E1321-18: Standard Test Method for Determining Material Ignition and Flame Spread Properties, West Conshohocken, PA, 2018. doi:10.1520/E1321-18.
- [32] J. Gales, K. Hartin, L. Bisby, *Structural Fire Performance of Post-tensioned Concrete Construction*, SpringerBriefs in Fire, New York, 2016. doi:https://doi.org/10.1007/978-1-4939-3280-1.
- [33] A.H. Buchanan, Fire performance of timber construction, *Prog. Struct. Eng. Mater.* 2 (2000) 278–289.
- [34] ASTM International, ASTM D143-14: Standard Test Method for Small Clear Specimens of Timber, West Conshohocken, PA, 2014. doi:10.1520/D0143-14.
- [35] S. Stanier, A. Take, J. Blaber, D. White, *GeoPIV-RG*, (2015).
- [36] J. Gales, M. Green, Optical Characterization of High Temperature Deformation in Novel Structural Materials, in: 14th Int. Conf. Fire Mater., San Francisco, CA, 2015: pp. 626–640.
- [37] K.L. Friquin, Material properties and external factors influencing the charring rate of solid wood and glue-laminated timber, *Fire Mater.* 35 (2011) 303–327. doi:10.1002/fam.1055.
- [38] F. Wiesner, F. Randmael, W. Wan, L. Bisby, R.M. Hadden, Structural response of cross-laminated timber compression elements exposed to fire, *Fire Saf. J.* 91 (2017) 56–67. doi:10.1016/j.firesaf.2017.05.010.

- [39] Standards Council of Canada, CAN/ULC-S101-14: Fire Endurance Tests of Construction and Materials, (2014).
- [40] International Organization for Standardization, ISO 834-11: Fire resistance tests -Elements of building construction - Part 11: Specific requirements for the assessment of fire protection to structural steel elements, (2014).